Statistical and Kinetic Approaches for Linear Low-Density Polyethylene Melting Modeling

A. Greco, A. Maffezzoli

Dipartimento di Ingeneria Dell'innovazione, Università degli Studi di Lecce, 73100 Lecce, Italy

Received 19 June 2002; accepted 23 August 2002

ABSTRACT: The aim of this study was to compare different models, either originating from literature or originally proposed in this study, for the interpretation of the melting behavior of polymers. In particular, these models, tested with a linear low-density polyethylene widely used in rotational molding, are suitable for coupling with energy balances in the study of polymer processing. We obtained the experimental data from differential scanning calorimetry (DSC) dynamic scans, assuming that the endothermic flux was related to the rate of melting of the polymer. The studied models were able to predict the broad melting temperature range typically observed during polymer melting with either a statistical or a kinetic approach. The two different approaches were compared with experimental DSC data. The analysis of model performances with complex thermal programs showed that the statistical approach could provide a more realistic representation of polymer melting. These models were particularly suitable in rotational molding, where the lack of any flow and, hence, of any crystalline orientation leads to a degree of melting determined by the actual temperature of the polymer. © 2003 Wiley Periodicals, Inc. J Appl Polym Sci 89: 289–295, 2003

Key words: polyethylene (PE); differential scanning calorimetry (DSC); melt; molding

INTRODUCTION

The great importance of the melting of polymers arises in many industrial problems. The melting process is usually observed over a broad temperature interval. This behavior is often attributed to the presence in the crystalline regions of lamellae of different thicknesses. In turn, for a given polymer, the lamellar thickness distribution depends on different factors, such as molecular weight, regularity of the chains, and especially crystallization conditions.[1–4] Furthermore, it is generally accepted that once the crystallization conditions are determined, the enthalpy and the temperature interval of melting do not depend on the particular conditions of the heating of the polymer.

The well-known Thomson–Gibbs equation states the dependence of the melting temperature of each crystallite on its thickness.[4] The particular behavior of macromolecular species has been attributed to the metastability of crystalline regions.[5–7] This is mainly due to the presence, on every crystal, of amorphous boundaries, acting as nuclei for melting.[8] Thus, when certain conditions of mobility are achieved for crystalline regions, there will be a strong tendency toward thermodynamic equilibrium, corresponding to the dissolution of lamellae.[9] Therefore, the melting process depends mainly on thermodynamic equilibrium and is not significantly affected by kinetics, as in the case of crystallization. Further, no superheating is possible for folded-chain crystals.[8]

In particular for linear low-density polyethylene (LLDPE), the broad melting peak during differential scanning calorimetry (DSC) scans is attributed to the presence of a broad branching distribution, which leads to a broad crystal thickness distribution. As a consequence, the cross-fractionation of chains according to the degree of branching leads to a sharp peak.[10]

The particular behavior of a polymer on melting is of interest when one deals with polymer processing. In particular in rotational molding, which is a virtually zero-shear rate process, the degree of melting is determined at each time of the process, just by the local temperature. This is true in each process where the sintering of semicrystalline polymers is involved, such as in rotational molding. To model this process, it could be very useful to establish a relationship between the degree of melting of the polymer and the temperature. With the assumption that kinetic effects play a secondary role in the heating rates of interest, the relationship between the equilibrium melting temperatures of crystallites and their thicknesses can be exploited.

Different techniques have been used to determine the lamellar thickness distribution for different grades of polyethylene. Among these are small angle X-ray scattering,[11–15] transmission electron microscopy,

Correspondence to: A. Maffezzoli (alfonso.maffezzoli@unile.it).
Contract grant sponsor: Centro di Progettazione, Design e Tecnologie dei Materiali (CETMA) (Brindisi, Italy).

Journal of Applied Polymer Science, Vol. 89, 289–295 (2003)

atomic force microscopy,[3] and DSC.[3,16,17] In contrast with these observations, a few attempts have been made to model the melting of polymeric materials with the proposed thermodynamic approach,[18] and a simple discontinuity of the specific heat[19] or models based on a kinetic approach are available in the literature.[20–22]

In this study, DSC was used to analyze the melting behavior of rotational-molding-grade LLDPE. The melting process was modeled with two different statistical distribution functions, one properly adapted for the studied LLDPE and a simple kinetic model. The relevant differences arising from the application of the kinetic and statistical approaches are highlighted.

EXPERIMENTAL

We used rotational-molding-grade LLDPE (Clearflex RM50, Polimeri Europa, Brindisi, Italy). The resin, in powder form, was studied as received in a differential scanning calorimeter (PerkinElmer DSC-7, Shelton, CT). Samples of about 5 mg were tested. For melting modeling purposes, DSC heating scans were run between 20 and 200°C at 10, 20, 30, and 50°C/min.

The output of the instrument was the specific heat flow versus time. After being corrected through baseline subtraction, the signal was numerically integrated through the second-order Runge–Kutta method to determine the partial integrals with respect to time:

$$H(t) = \int_{t_0}^{t} \left(\frac{dH}{dt} - BL \right) dt \tag{1}$$

where $H(t)$ is the heat absorbed at time t to promote polymer melting, t_0 is the initial time of the scan, and BL is the baseline. dH/dt is the output of DSC instrument. The melting enthalpy can also be obtained as a function of temperature through a variable exchange:

$$H(T) = \frac{1}{\beta} \int_{T_0}^{T} \left(\frac{dH}{dt} - BL \right) dT \tag{2}$$

where T_0 is the starting temperature and β is the scanning rate.

The degree of transition (X_m) was defined as

$$X_m(t) = H(t)/H_T$$
$$X_m(T) = H(T)/H_T \tag{3}$$

where H_T is a reference value, which was assumed to be the total heat absorbed in the melting process. With these assumptions, X would range in the interval [0, 1].

For kinetic modeling, the rate of transition was evaluated as

$$dX_m(t)/dt = (1/H_T)[dH(t)/dt) \tag{4}$$

whereas the distribution of melting temperatures was evaluated as

$$dX_m(T)/dt = (1/H_T)[dH(T)/dt) \tag{5}$$

RESULTS AND DISCUSSION

Melting models

We made a comparison between a kinetic approach and two different statistical approaches. The kinetic equation adopted was[21]

$$\frac{dX_m}{dt} = K_m(1 - X_m)^{n_m} \tag{6}$$

where X_m is the molten polymer volume fraction, n_m is the kinetic order, and K_m is the kinetic constant, which is given by an Arrhenius-type expression:

$$K_m = K_{m0} \exp(-E_{m0}/RT) \tag{7}$$

where R is the universal gas constant, T is the temperature, K_{m0} is a pre-exponential factor, and E_{m0} is the activation energy for the crystal melting process.

The statistical approach was based on the assumption that the DSC melting peak (once the baseline was subtracted) could be regarded as a statistical distribution of melting temperatures resulting from a distribution of lamellar thickness.[1,3,4,18] Therefore, the integral curve of the DSC melting peak, defined as the degree of melting (X_m), was regarded as the cumulative distribution curve. The statistical model, proposed by Nichols and Robertson[18] and modified by Chen et al.[23] was

$$\frac{dX_m}{dT}(T) = N(1 - p^2)\left[\left(T_p - \frac{1}{\ln p} - T \right) p^{(T_p - (1/\ln p) - T)} - \left(T_p - \frac{1}{\ln p} - T_{on} \right) p^{(T_p - (1/\ln p) - T_{on})} \right] \tag{8}$$

where p is the curve shape factor, N is a scale factor, T_{on} is the observed temperature at the onset of melting, and T_p is the peak temperature related to the maximum melting temperature from $T_p = T_m^* + 1/\ln p$, where T_m^* is the temperature at the end of melting.

The distribution defined in eq. (8) is zero at the onset of melting but is different from zero at T_m^*. With $dX_m/dT(T_m^*)$ very close to zero, it can be considered null.

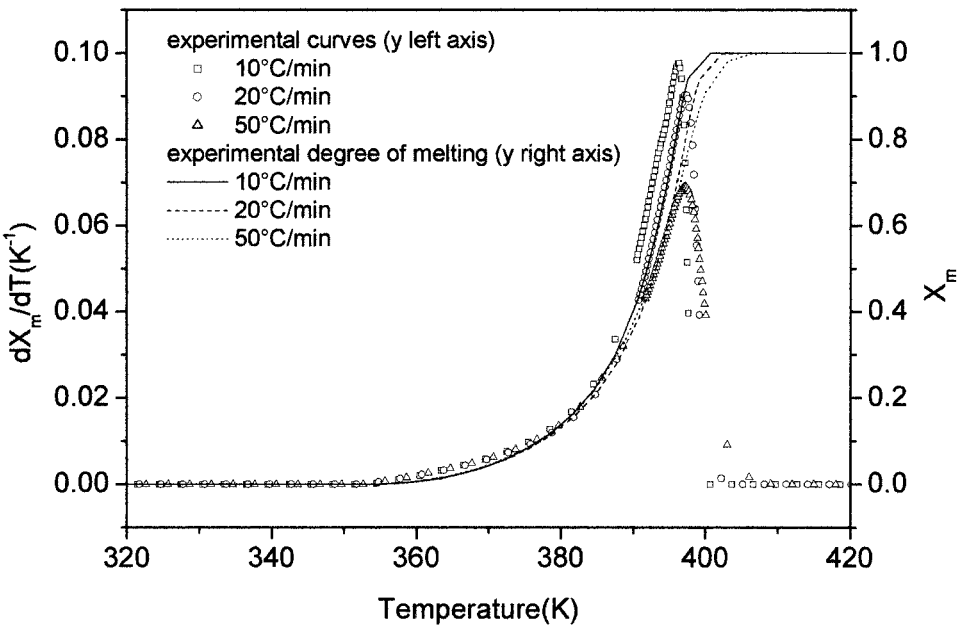

Figure 1 Differential and integral DSC melting curves for LLDPE at different heating scans.

By the analytical integration of eq. (8), the cumulative curve of the melting temperatures was obtained. We determined the integration constant by properly setting the integration limits. To force the cumulative curve to 0 and 1 at the beginning and end of melting, respectively, this expression had to be used, which became more complex. A simplified expression, which gives $X_m(T_{on}) = 0$ and $X_m(T_m^*) \cong 1$, is given by

$$X_m(T) = (\ln p)^2 \left\{ \left[\frac{T - \left(T_p - \frac{1}{\ln p}\right)}{\ln p} + \frac{1}{(\ln p)^2} \right] p^{T_m^* - T} - \left[\frac{T_{on} - \left(T_p - \frac{1}{\ln p}\right)}{\ln p} + \frac{1}{(\ln p)^2} \right] p^{T_p - (1/\ln p)T_{on}} - \left(T_p - \frac{1}{\ln p} - T_{on}\right)(T - T_{on}) p^{T_p - (1/\ln p)T_{on}} \right\} \quad (9)$$

Because T_p and T_{on} could be experimentally determined, only one parameter needed to be determined, p. It is important to observe that this function could not be used for $T > T_m^*$; after this point, dX_m/dT became negative, reaching very low values and thus leading the cumulative curve to negative values. The equation could, therefore, be used only for temperature values lower than T_m^*; for higher values, the distribution needed to be forced to 0. The same applied for $T < T_{on}$.

To improve the prediction capability of the statistical approach, a different function was used. The cumulative curve was represented through a sigmoidal growth curve,[24,25] known as the Richards function:[26,27]

$$X_m(T) = \{1 + (d - 1) \exp[-k_{mb}(T - T_c)]\}^{1/(1-d)} \quad (10)$$

When this expression is derived, the melting temperature distribution can be modeled as

$$\frac{dX_m}{dT}(T) = k_{mb}\{\exp[-k_{mb}(T - T_c)]\} \times (1 + (d - 1)\exp[-k_{mb}(T - T_c)]\}^{d/(1-d)} \quad (11)$$

where T_c is the temperature corresponding to the peak of the signal, which is regarded as the most probable melting temperature; k_{mb} is an intensity factor related to the sharpness of the distribution; and d is the shape factor. An increase of k_{mb} resulted in an increase of the peak value and in a lower dispersion around the most probable value. Increasing d resulted in a higher dispersion of melting temperatures at lower values than the most probable one. The effects of k_{mb} and d on the

TABLE I
Melting Enthalpies and Peak Temperatures from the DSC Experiments at Different Heating Rates

β (°C/min)	Melting enthalpy (J/g)	Peak temperature (K)
10	118.5	396.216
20	119.1	397.283
30	115.9	398.254
50	118.5	400.887

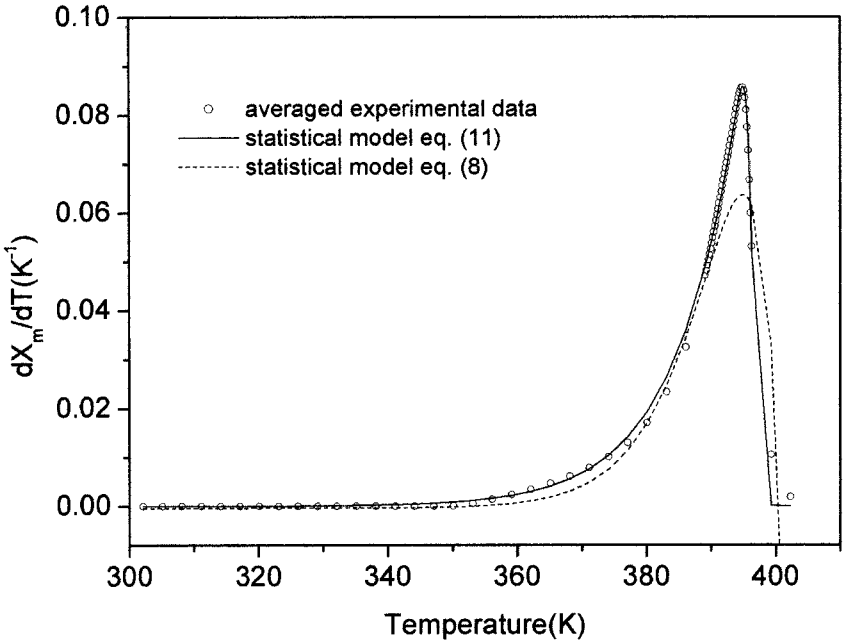

Figure 2 Model prediction of melting DSC endotherms according to eqs. (8) and (11).

peak height could be better understood by the calculation of the maximum value of the distribution occurring at T_c:

$$\frac{dX_m}{dT}(T_c) = \left.\frac{dX_m}{dT}\right|_{\max} = k_{mb} d^{d/(1-d)}$$

A prominent advantage of eq. (11) with respect to eq. (8) in polymer processing modeling is its ability to provide a differential expression capable of going to zero outside the melting range.

Comparison with experimental data

In Figure 1, the DSC thermograms obtained at different heating scans are shown. According to ref. 8, the effects of superheating in polymer melting are related to the presence of extended crystalline chains. In such

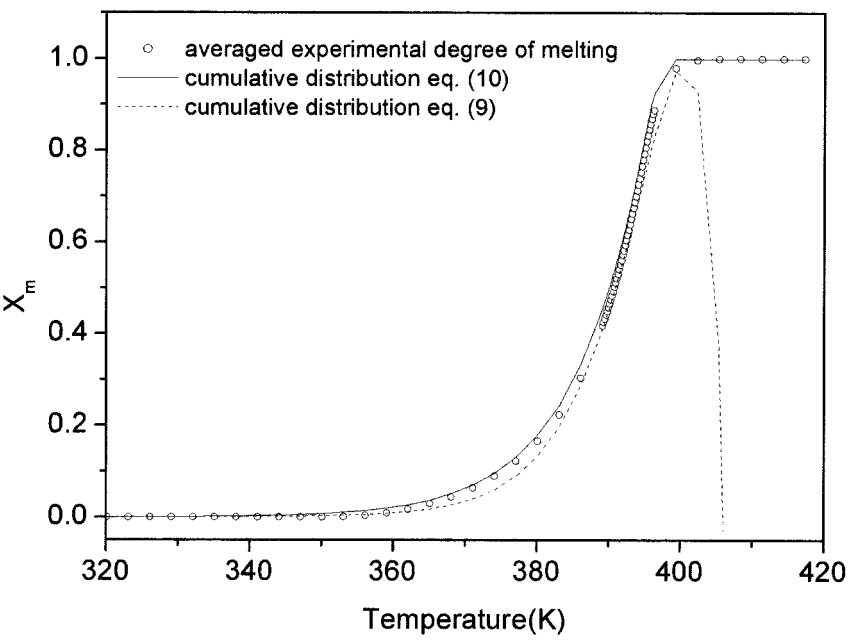

Figure 3 Model prediction of melting integral curves according to eqs. (9) and (10).

TABLE II
Parameters for Melting Modeling Obtained from the Nonlinear Regression of the Experimental Data

Statistical model (8)	Statistical model (11)	Kinetic model (6), (7)
p[exp(1/K)] = 0.84038	$K_{mb}(1/K)$ = 2.24902	$K_{m0}(1/s)$ = exp(37.5)
$T_0(K)$ = 353	d = 22.70037	$E_{m0}/R(K)$ = 16,300
$T_p(K)$ = 394.962	$T_c(K)$ = 394.962	n_m = 0.44

cases, at different heating rates, the melting behavior of the polymer changes, and kinetic effects are involved. This behavior is due to the increased stability of the extended chain crystals with respect to folded-chain crystals.[8] Another phenomenon that is related to the scanning rate is annealing of semicrystalline polymers.[18] In this case, when the polymer begins to melt, the increased mobility of amorphous regions is responsible for the growth of thicker crystals. Two endothermic peaks sometimes associated with an exothermic peak are detected in the DSC scans. As evident in Figure 1, none of these effects was seen in our experiments.

The DSC melting peaks obtained at different heating rates, shown in Figure 1, could not be described with a symmetric statistical distribution, such as the Gaussian one proposed by Crist and Mirabella.[17] The experimental data showed a broad dispersion for values of temperature lower than the most probable one. The integral curves for the different scanning rates are also reported in Figure 1.

The shapes of the curves in Figure 1 are essentially the same, and the temperature shift (peak temperature in Table I) was attributed to thermal lag effects in the DSC oven.[3,28] However, the melting enthalpy did not depend on the heating rate, as shown in Table I.

Following the procedure proposed by Zhou and Wilkes,[3] the actual distribution was obtained by the extrapolation of the experimental melting peaks at zero heating rate, according to an exponential function:

$$\ln T_p = A + B^* dT/dt$$

The curves were then shifted to a new position corresponding to T_p = 394.96. No attempt was made to correct the shape of the distribution because the relation to the heating rate was complex,[28] and the curves were characterized by similar shapes after the extrapolation procedure.

The extrapolated curves were simultaneously fitted according to the two different statistical models of eqs. (8) and (11). A comparison between experimental data averaged over the studied heating rates and models prediction is shown in Figure 2.

In Figure 3, the cumulative curves obtained with numerical integration are shown. As shown in this figure, the strongly negative values that the function

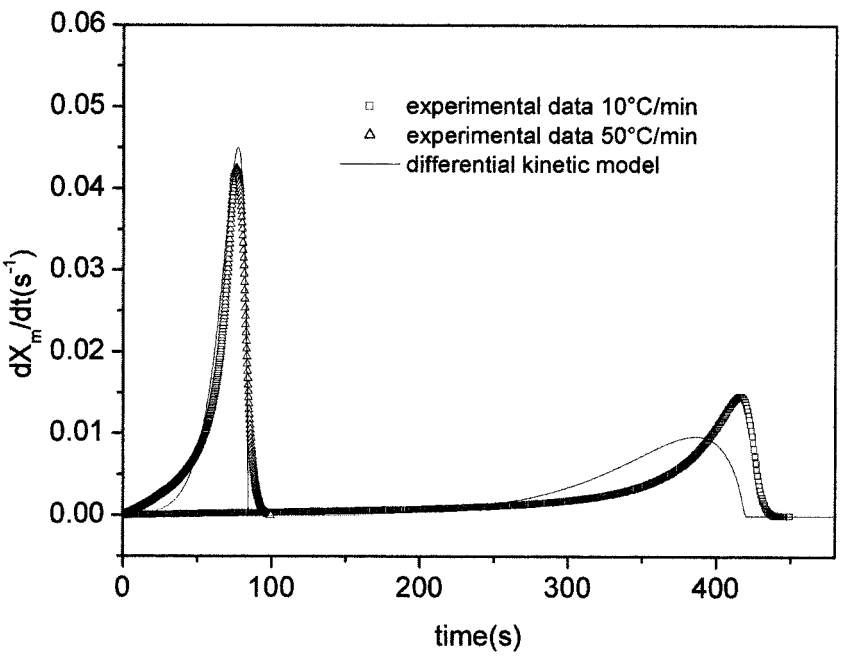

Figure 4 Model prediction of melting DSC endotherms according to eqs. (6) and (7).

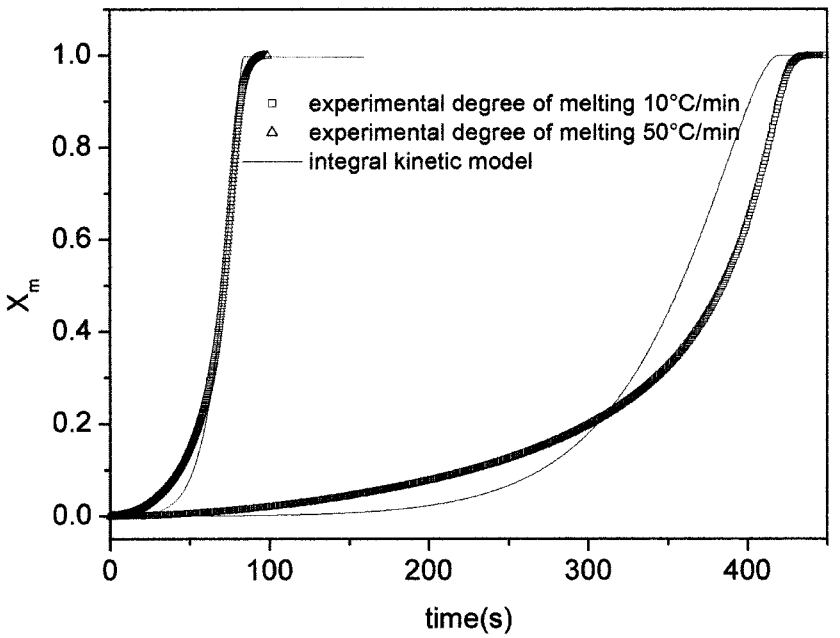

Figure 5 Model prediction of melting integral curves from the numerical integration of eqs. (6) and (7).

of eq. (8) took for temperatures higher than T_m^* forced the integral curve to values without physical meaning. So the distribution given from eq. (8) needs to be set to 0 above T_m^*.

The parameters obtained from nonlinear regression for the three different models are shown in Table II.

The melting process was also modeled through the kinetic equation , which together with eq. (7), gives the rate of conversion as a function of time and temperature. The numerical integration of the melting rate gives at any time the degree of melting. In Figures 4 and 5, the differential and the integral curves, respectively, obtained for the kinetic model of melting are shown. Here, one can see that a kinetic model could not predict the melting behavior of LLDPE in a wide range of heating rates.

The two different approaches were compared with a thermal history given by a heating scan at 10°C/min; an isothermal step at 120°C, where melting had begun but was not yet completed; and further heating at

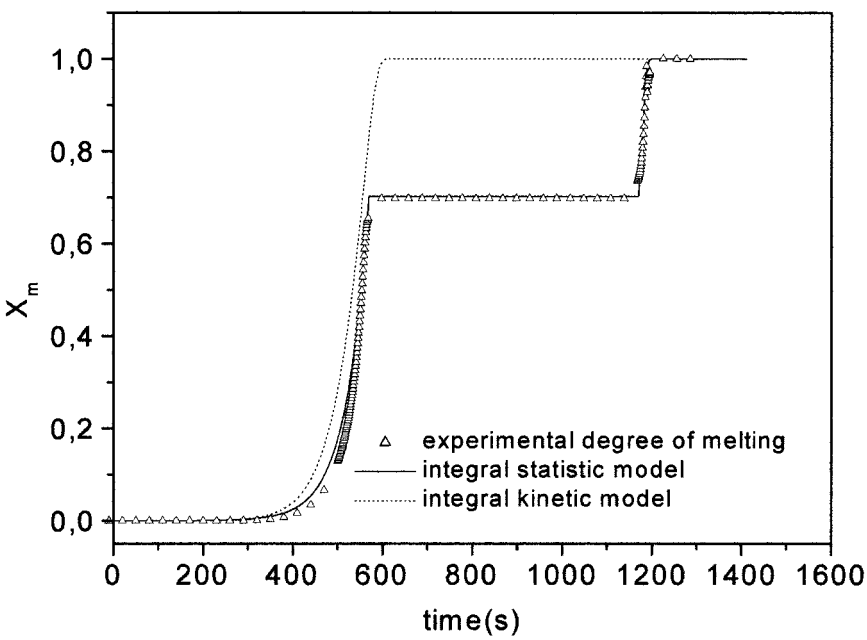

Figure 6 Comparison of kinetic and statistical model predictions for a heating scan at 10°C/min followed by an isothermal step at 120°C and further heating at 10°C/min to 150°C.

10°C/min to complete melting (150°C). The degree of melting resulting from this temperature program is shown in Figure 6, compared with model predictions according to the kinetic model and the proposed statistical model with the parameters given in Table II.

The experimental data showed that no melting took place when the sample was kept at 120°C. This was a further indication that the process was not time dependent and that melting behavior of the sample was determined just by its temperature; this supports the statistical approach. In fact, the statistical model fit the experimental data well, predicting no melting during the isothermal step at 120°C, which was confirmed by experimental observation. The kinetic model, also reported in Figure 6, predicted a rate of melting different from 0 once melting began, even if the temperature was kept constant, which was in contrast with our experimental observations. This could be explained by the fact that once melting has begun and temperature is kept constant, k_m is constant, and the polymer continues to melt, according to eq. (6), until the melting rate goes to zero. However, if eq. (11) is used, at a constant temperature $dX_m/dt = (dX_m/dT)(dT/dt) = 0$ because in isothermal conditions, $dT/dt = 0$. Once the temperature is raised again, $dT/dt > 0$, and melting continues.

CONCLUSIONS

In this study, DSC was used to analyze the melting behavior of a rotational-molding-grade LLDPE. The DSC melting peak, regarded as a statistical distribution of lamellar crystal thicknesses, was modeled with a distribution function. A properly developed statistical model was compared with formerly proposed kinetic and statistical models. The application of the statistical and kinetic approaches to a thermal history more complex than a simple heating ramp led to completely different results. Experimental data compared well only with the statistical model, showing the presence of unmolten crystals when the temperature was kept constant in the melting range. Only further heating led to complete melting in both the experimental DSC data and the statistical model predictions. However, the kinetic model predicted complete melting during an isothermal step in the melting temperature range. This statistical approach can be a valuable tool for modeling heat-transfer phenomena occurring in rotational molding.

The authors thank John Vlachopoulos for his useful discussions.

References

1. Lu, L.; Alamo, R. G.; Mandelkern, L. Macromolecules 1994, 27, 6571.
2. Marega, C.; Marigo, A.; Cingano, G.; Zannetti, R.; Paganetto, G. Polymer 1996, 37, 5549.
3. Zhou, H.; Wilkes, G. L. Polymer 1997, 38, 5735.
4. Mallapragada, S. K.; Peppas, N. A. In Proceedings of the American Chemical Society, Division of Polymeric Materials, Science and Engineering, Fall Meeting, November 1995, Chicago, IL.
5. Keller, A. Macromol Symp 1995, 98, 1.
6. Wunderlich, B. Macromolecular Physics. Vol. 3. Crystal Melting; Academic: New York, 1976; pp 12–14.
7. Keller, A.; Hikosaka, M.; Rastogi, S.; Toda, A.; Barham, P. J.; Goldbeck-Wood, G. J Mater Sci 1994, 29, 2579.
8. Hellmuth, E.; Wunderlich, B. J Appl Phys 1965, 36, 3039.
9. Mathot, V. B. F.; Scherremberg, R. L.; Pijpers, T. F. J. Polymer 1998, 39, 4541.
10. Bodor, G.; Dalcolmo, H. J.; Schroter, O. Colloid Polym Sci 1989, 267, 480.
11. Blundell, D. J. Polymer 1978, 19, 1258.
12. Alberola, N.; Cavaille, J. Y.; Perez, J. J Polym Sci Part B: Polym Phys 1990, 28, 569.
13. Darras, O.; Seguela, R. Polymer 1993, 34, 2946.
14. Lee, Y. D.; Phillips, P. J.; Lin, J. S. J Polym Sci Part B: Polym Phys 1991, 29, 1235.
15. Hosoda, S. Polym J 1988, 20, 383.
16. Wlochowicz, A.; Eder, M. Polymer 1984, 25, 1268.
17. Crist, B.; Mirabella, F. J. J Polym Sci Part B: Polym Phys 1999, 37, 3131.
18. Nichols, M. E.; Robertson, R. E. J Polym Sci Part B: Polym Phys 1992, 30, 755.
19. Tadmor, Z.; Gogos, C. G. Principles of Polymer Processing; Wiley: New York, 1979; p 276.
20. Czornyj, G.; Wunderlich, B. J Polym Sci Polym Phys Ed 1977, 15, 1905.
21. Maffezzoli, A.; Kenny, M. J.; Nicolais, L. In Proceedings of the 10th Intl. SAMPE Conference, Materials and Processing—Move into the 90s, Birmingham, UK; Benson, S.; Cook, T.; Trewin, E.; Turner, R. M., Eds.; Elsevier: Amsterdam, Holland, 1989; p 133.
22. Ageorges, A.; Ye, L.; Mai, Y. W. Compos A 1998, 29, 921.
23. Chen, H. L.; Hwang, J. C.; Chen, C. C. Polymer 1996, 37, 5461.
24. Drakopoulos, J. A. Fuzzy Sets Syst 1995, 76, 349.
25. Drakopoulos, J. A. Fuzzy Sets Syst 1998, 99, 57.
26. Tsoularis, A. Res Lett Inf Math Sci 2001, 2, 23.
27. Seber, G. A. F.; Wild, C. J. Nonlinear Regression; Wiley: New York, 1989; pp 332–337.
28. Plummer, C. J. G.; Kausch, H. H. Polym Bull 1996, 36, 355.